

## Effect of the anchoring group in porphyrin sensitizers: phosphonate versus carboxylate linkages

Christine STERN<sup>1</sup>, Alla BESSMERTNYKH LEMEUNE<sup>1</sup>, Yulia GORBUNOVA<sup>2,3</sup>,  
Aslan TSIVADZE<sup>2,3</sup>, Roger GUILARD<sup>1,\*</sup>

<sup>1</sup>Institut de Chimie Moléculaire de l'Université de Bourgogne (ICMUB), UMR CNRS 6302, Dijon, France

<sup>2</sup>A.N. Frumkin Institute of Physical Chemistry and Electrochemistry, Russian Academy of Sciences,  
Moscow, Russia

<sup>3</sup>N.S. Kurnakov Institute of General and Inorganic Chemistry, Russian Academy of Sciences, Moscow, Russia

Received: 16.06.2014 • Accepted: 19.07.2014 • Published Online: 24.11.2014 • Printed: 22.12.2014

**Abstract:** Porphyrins are an important family of organic chromophores that have attracted attention as photosensitizers in TiO<sub>2</sub>-based dye-sensitized solar cells (DSSCs). This brief review is dedicated to comparative studies of phosphonic and carboxylic acid anchoring groups for attachment of porphyrin sensitizers on semiconductors or conductors surface. Here we have selected some representative examples of recently described phosphonate/carboxylate porphyrins with the aim to demonstrate that porphyrin phosphonate should be a promising anchoring group for such systems.

**Key words:** Phosphoryl porphyrins, carboxylate porphyrins, dye-sensitized solar cells, photovoltaic performance

### 1. Introduction

Numerous methods for grafting porphyrins and phthalocyanines onto the surface of organic or inorganic solids have been described with the view of designing novel materials to prepare supported catalysts, chemically modified electrodes, or medical applications. In recent years dye sensitization of mesoporous thin films of wide band gap semiconductors has been extensively studied for photovoltaic energy. In typical dye-sensitized solar cells (DSSCs) for example, it has been shown that the properties and efficiency of the electron transfer step at the dye-TiO<sub>2</sub> interface depend on the number and the nature of the anchoring groups.<sup>1–8</sup>

In a previous review covering the synthesis of porphyrin derivatives possessing a pentavalent phosphorus functional group we have shown that the metal-mediated C–P bond forming reactions have been recently used to prepare new series of porphyrins and can be successfully applied to the synthesis of essential precursors possessing phosphonate moieties as anchoring groups.<sup>9</sup> These A<sub>4</sub>, A<sub>3</sub>B, A<sub>2</sub>B<sub>2</sub> *meso*- and *β*-porphyrins exhibit a priori new and novel chemical and physical properties. More specifically it was already shown that the self-aggregation of metal complexes of (dialkoxy)porphyrins observed in solution and in solid state affords discrete supramolecular architectures or 1D and 2D networks.<sup>10–15</sup>

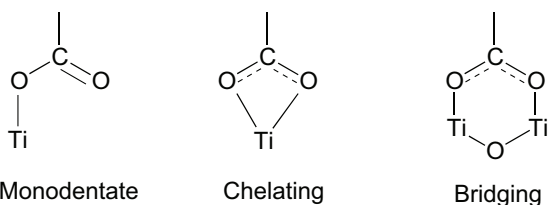
This brief review is dedicated to comparative studies of phosphonic and carboxylic acid groups for attachment of porphyrin sensitizers on semiconductors or conductors. The aim of the review is to demonstrate on the examples of recently described phosphonate porphyrins that the motif in such type of compounds should be a promising anchoring group for porphyrin-sensitized solar cells.

\*Correspondence: roger.guilard@u-bourgogne.fr

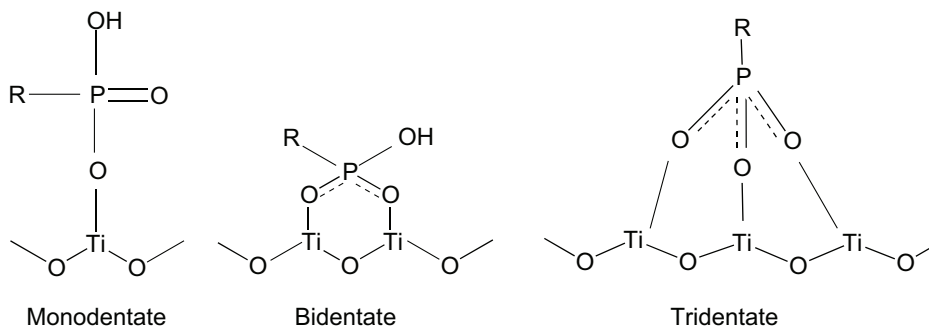
## 2. Anchoring groups used in porphyrin series

Various anchoring groups have been used to graft porphyrins (Scheme 1). Porphyrins substituted at the *meso*- and  $\beta$ -positions with a carboxylic group have been described and their anchoring has been extensively studied.<sup>1,5,16</sup> Three different modes of grafting of the carboxylate motif were a priori observed on TiO<sub>2</sub>, i.e. monodentate, chelating, and bridging modes (Scheme 1).<sup>17</sup>

### Carboxylate groups



### Phosphonate groups



Scheme 1.

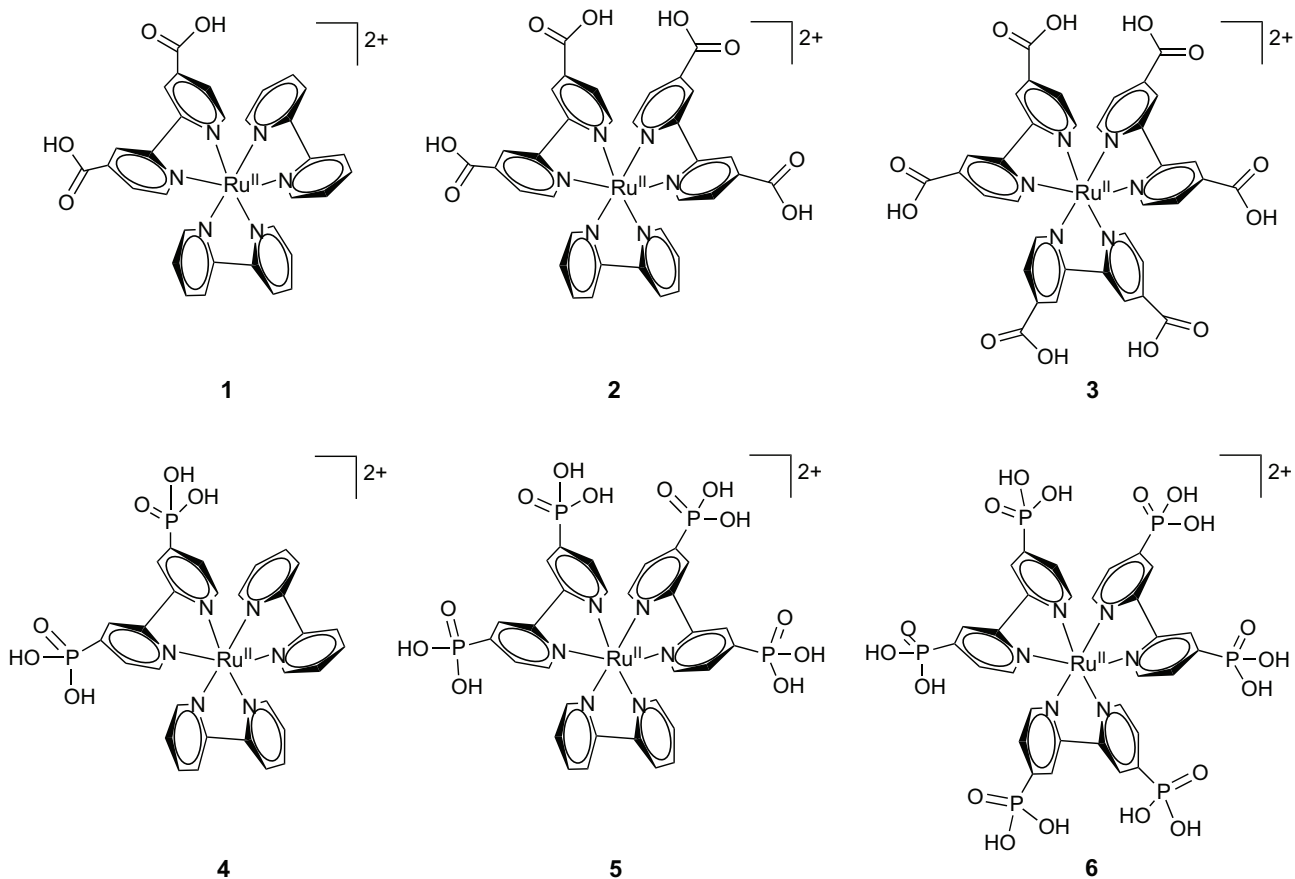
Another important anchoring group is phosphonic acid but the studies dedicated to this anchoring group are more limited in the porphyrin series. However, it is known that the possible binding modes for organophosphonates are monodentate, bidentate, and tridentate.<sup>18</sup>

Even though this review is not devoted to studies of other anchoring groups, it is necessary to mention that other functions were used to graft porphyrins on a support; these are the trialkoxysilanes and silatranes, pyridines, 8-hydroxyquinolines, and sulfonic acids.<sup>19–22</sup>

## 3. Carboxylate versus phosphonate linkages in non-porphyrin series

These data are related to DSSCs, i.e. a dye coated porous TiO<sub>2</sub> electrode and their photoelectrochemical performances. Derivatives of Ru-bipyridyl complexes substituted by di-, tetra-, or hexacarboxylate or di-, tetra-, or hexaphosphonate (**1–6**) have been studied in details (Scheme 2, Table 1).<sup>23,24</sup>

In a first study Choi and coworkers showed that the complex **3** (i.e. the hexacarboxylate) is attached through a bidentate coordination, not a monodentate coordination of 2 anchoring groups and the complex **4** (i.e. the diphosphonate) is bound to the surface via 2 bidentate or tridentate acid groups (Scheme 1).<sup>23</sup> The authors compared the reactivity and stability of the 2 sensitized TiO<sub>2</sub> photocatalysts (Pt/TiO<sub>2</sub>/**3** versus Pt/TiO<sub>2</sub>/**4**) in water. Despite the fact that **4** has a lower visible light absorption than **3** and both photocatalysts are not stable enough under the studied conditions, the phosphonate group appears to be a better ruthenium sensitizer linkage to the TiO<sub>2</sub> surface than the carboxylate group for applications dealing with aqueous media.



Scheme 2.

**Table 1.** Photoelectrochemical performances of the sensitized TiO<sub>2</sub> electrodes under visible light-irradiation.

Ru complex	Saturated surface coverage (nmol/cm <sup>2</sup> )	V <sub>OC</sub> (V)	J <sub>SC</sub> (mA/cm <sup>2</sup> )	FF	PCE (%) <sup>a</sup>
1	41	0.51	0.30	0.47	0.1
2	43	0.71	1.18	0.71	0.8
3	116	0.49	0.34	0.44	0.1
4	45	0.67	1.36	0.68	0.8
5	41	0.53	0.22	0.58	0.09
6	38	0.80	2.87	0.62	1.9

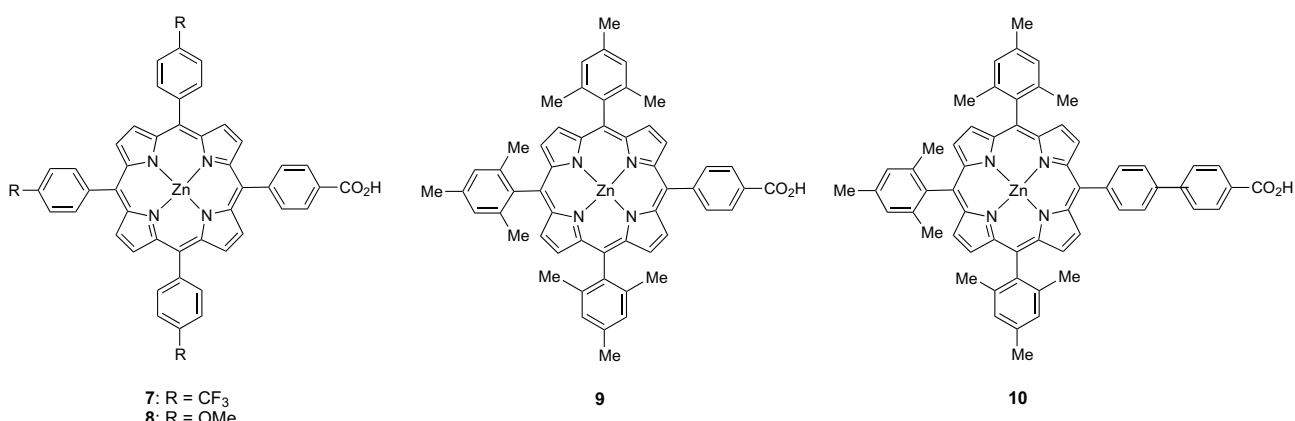
<sup>a</sup> Measured on the basis of the incident light (420–645 nm) intensity of 74 mW/cm<sup>2</sup>.

In 2006 the same group studied the effect of the number of anchoring groups in Ru-bipyridyl complexes on their binding to a TiO<sub>2</sub> surface and the photoelectrochemical performances of the sensitized electrodes.<sup>24</sup> The studied derivatives were the 6 Ru-bipyridyl complexes (**1–6**) bearing di-, tetra-, or hexa-carboxylates and -phosphonates. The same modes of coordination onto the surface were observed as previously detailed, i.e. bidentate coordination for carboxylate groups, and bidentate and tridentate for phosphonate groups. It was proven that the surface binding on TiO<sub>2</sub> and the overall cell performances were strictly dependent on the number and the nature of the anchoring groups. In carboxylate series the most efficient surface binding mode

was observed for the tetrasubstituted system (**2**), which gave the best cell performances even though it had the lowest visible light absorption. It is remarkable to note that the photoelectrochemical behavior of phosphonate–TiO<sub>2</sub> systems did not depend on the number of phosphonate anchoring groups due to the stronger binding capability of the phosphonate group. Consequently, the overall cell performance in the phosphonate series varies only according the visible light absorption, which is dependent on the number of phosphonate groups.

#### 4. Anchoring carboxylic acid groups at the *meso* position of porphyrin dyes

Imahori and coworkers have studied the effects of varying *meso*-aryl anchoring moiety for a series of *meso*-tetraaryl zinc porphyrins on porphyrin-sensitized TiO<sub>2</sub> cells (Scheme 3).<sup>25</sup> Other parameters such as the immersing solvents and the porphyrin adsorption times have also been investigated (Table 2).



**Scheme 3.**

**Table 2.** Photovoltaic performance of dye-sensitized solar cells.

Cells	Solvent	IPCE (APCE) %		$J_{SC}$ (mA/cm <sup>2</sup> )	$V_{OC}$ (mV)	FF	PCE (%)
		420 nm	560 nm				
TiO <sub>2</sub> / <b>7</b>	<i>t</i> -BuOH/MeCN	53 (53)	44 (48)	6.4	0.68	0.64	2.8
	MeOH	58 (58)	43 (45)	6.6	0.67	0.68	3.0
TiO <sub>2</sub> / <b>8</b>	MeOH	65 (65)	42 (44)	8.3	0.66	0.63	3.5
TiO <sub>2</sub> / <b>9</b>	<i>t</i> -BuOH/MeCN	63 (63)	52 (56)	7.6	0.69	0.64	3.4
	MeOH	76 (76)	58 (60)	9.4	0.76	0.64	4.6
TiO <sub>2</sub> / <b>10</b>	<i>t</i> -BuOH/MeCN	57 (57)	40 (41)	5.6	0.64	0.66	2.4

The authors have shown that the photovoltaic performance of the porphyrin-sensitized TiO<sub>2</sub> cell was greatly dependent on the steric bulkiness around the macrocycle, the electronic coupling between the porphyrin core and the TiO<sub>2</sub> surface, the immersing solvent, and the immersing time. The highest cell performance was observed with a protic solvent (CH<sub>3</sub>OH) and a short immersion time (1 h). These results are in contrast with the data obtained for Ru dye-sensitized TiO<sub>2</sub> cells, which are not crucially dependent on the immersing solvent and the immersing time. The 5-(4-carboxyphenyl)-10,15,20-tris(2,4,6-trimethylphenyl)porphyrinatozinc(II) **9** showed the highest cell performance, with a power conversion efficiency of 4.6%. These data were rationalized by the increase in the porphyrin aggregation with increasing immersing time and the large steric repulsion between the *ortho*-methyl substituents and the porphyrin ring of **9**. The steric repulsion induces an orthogonal

orientation of the phenyl group against the porphyrin ring, resulting in rather well separated porphyrin cores of the mesityl groups reducing the intermolecular interaction between the porphyrins on the  $\text{TiO}_2$  surface. Such a geometry leads to a decrease in nonradiative processes from the porphyrin excited singlet state favoring an increase in the PCE.

The effect of the orientation of the porphyrin sensitizer onto the  $\text{TiO}_2$  surface has been studied in detail by D'Souza and coworkers using free base and zinc porphyrins bearing a carboxyl anchoring group at the *para*-, *meta*-, or *ortho*-positions of the *meso*-aryl substituents (Figure).<sup>26</sup>

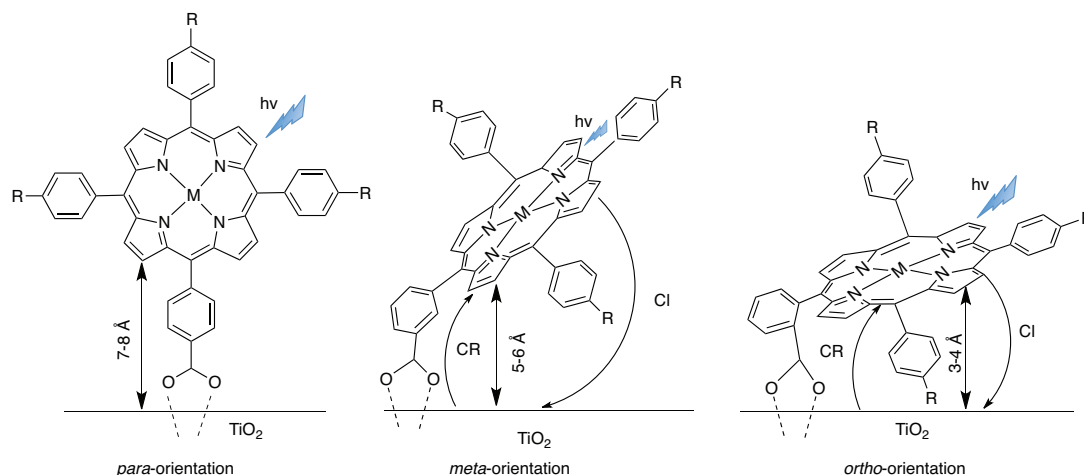


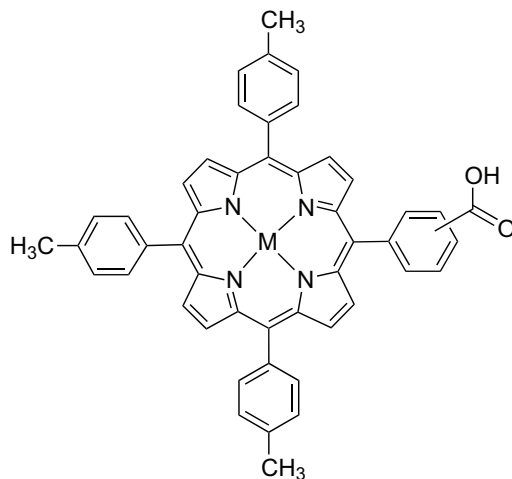
**Figure.** Relative orientation of carboxyphenyl functionalized porphyrins adsorbed on  $\text{TiO}_2$  surface (CI: charge injection; CR: charge recombination).

Taking into account the rigid bidentate binding of the carboxylic group on  $\text{TiO}_2$ , the authors suggested that the *para*-carboxyphenyl substituent locates the porphyrin  $\pi$ -system orthogonal to the  $\text{TiO}_2$  surface, the *meta*-carboxyphenyl group locates the  $\pi$ -system at an angle ( $50\text{--}80^\circ$ ), and the *ortho*-carboxyphenyl spacer brings the  $\pi$ -system into the proximity of the  $\text{TiO}_2$  surface. The *meta*-derivatives should favor through-bond and through-space interactions, while the *ortho*-derivatives should facilitate stronger through-space interactions. The data observed for these 3 free bases (**11–13**) and their zinc complexes (**14–16**) are summarized in Table 3.

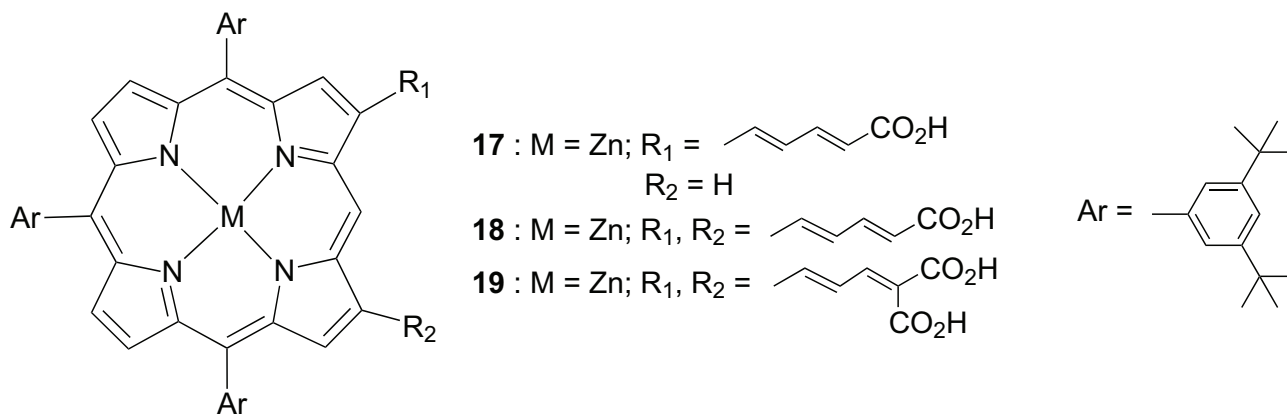
These data show that the porphyrins anchored to the mesoporous  $\text{TiO}_2$  with a *para*- and a *meta*-carboxy group present stronger photovoltaic performances compared to the corresponding *ortho*-derivative. Indeed, a fast charge recombination time through-space charge transfer was observed for the *ortho* derivatives. Moreover, stronger performances were observed using zinc porphyrins **14–16** compared to the corresponding free bases **11–13**.

## 5. Anchoring carboxylic groups at the $\beta$ position of porphyrins

Park et al. have studied the electronic properties and photoconversion efficiency of DSSCs based on zinc tetraaryl porphyrins  $\beta$ -functionalized with unsaturated carboxylic acid adsorbed onto a  $\text{TiO}_2$  nanocrystalline surface.<sup>27</sup> Among them, porphyrins doubly functionalized with a dienic fragment bearing 2 carboxylate groups **19** demonstrate the higher photovoltaic performances (Table 4).

**Table 3.** Photovoltaic performance of DSSCs based porphyrins **11–16** with liquid electrolyte (M = H<sub>2</sub>, Zn).

Dye	$J_{SC}$ (mA/cm <sup>2</sup> )	$V_{OC}$ (V)	FF	PCE (%)	Amount (mol/cm <sup>2</sup> )
<b>N719</b>	18.13	0.62	0.66	7.39	
<b>11</b>	1.26	0.45	0.75	0.42	
<b>14</b>	6.67	0.59	0.79	3.13	$1.76 \times 10^{-7}$
<b>12</b>	2.06	0.48	0.72	0.71	
<b>15</b>	8.42	0.65	0.82	4.17	$2.19 \times 10^{-7}$
<b>13</b>	0.31	0.45	0.83	0.11	
<b>16</b>	1.01	0.51	0.71	0.37	$1.32 \times 10^{-7}$

**Table 4.** Photoelectrochemical data of the porphyrin sensitized solar cells.<sup>a</sup>

Compound	IPCE (%) (nm)		$J_{SC}$ (mA/cm <sup>2</sup> )	$V_{OC}$ (V)	FF	PCE (%)
	Soret	Q-band				
<b>17</b>	51.6 (450)	23.0 (580)	6.20	0.54	0.62	2.08
<b>18</b>	53.6 (470)	27.3 (590)	6.74	0.56	0.62	2.37
<b>19</b>	60.1 (450)	21.8 (590)	8.38	0.59	0.62	3.03

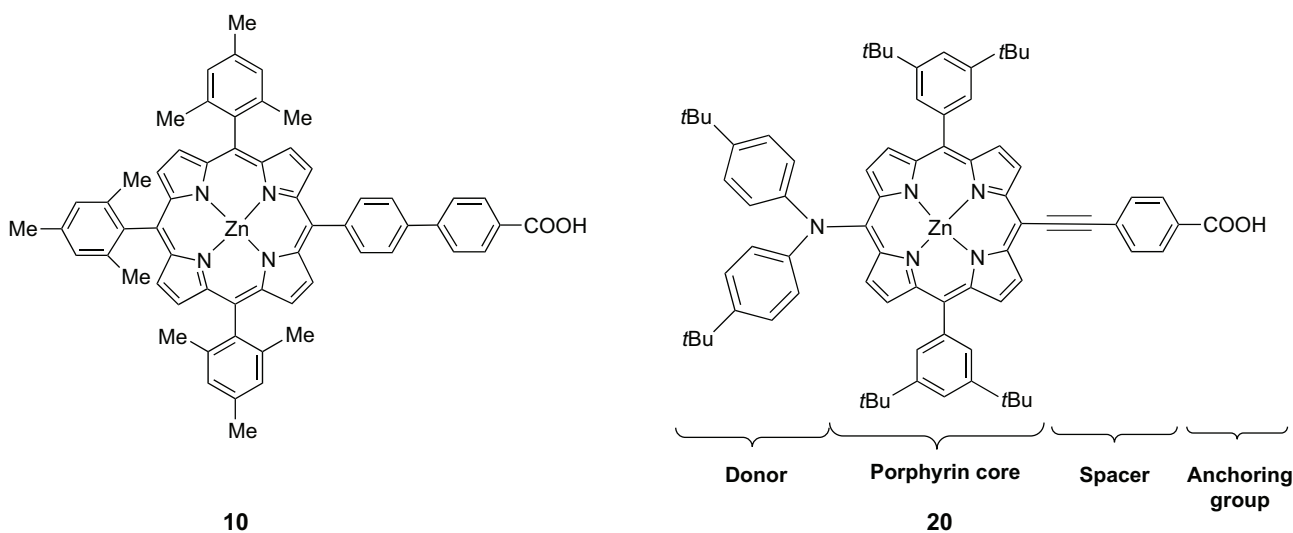
<sup>a</sup> Overall conversion efficiency parameters were measured in the light condition of 100 mW/cm<sup>2</sup> illumination.

The authors observed H-type interactions in porphyrin systems indicating highly packed monolayers of porphyrins on the TiO<sub>2</sub> surface. The coupling through the bridge is a key parameter in the charge injection process. Another parameter is the moderate distance between the adsorbed porphyrin and the

TiO<sub>2</sub> nanocrystalline, which induces a better performance in photoelectrochemical conversion due to the reduced rate of charge recombination processes. Finally, the presence of the malonic acid moieties in **19** (which is a stronger electron-withdrawing fragment as compared to mono-carboxylates) induces more efficient electron injection, resulting in the largest conversion efficiency of 3.03%.

## 6. Push-pull carboxylic porphyrin

As already described, Imahori and coworkers have prepared the dye **10** to decrease the formation of dye aggregate on the semiconductor surface.<sup>25</sup> To improve the charge separation in the dye, Diau and coworkers have added an efficient pushing group at the *meso*-position of the porphyrin macrocycle to form **20** (Scheme 4).<sup>28</sup>

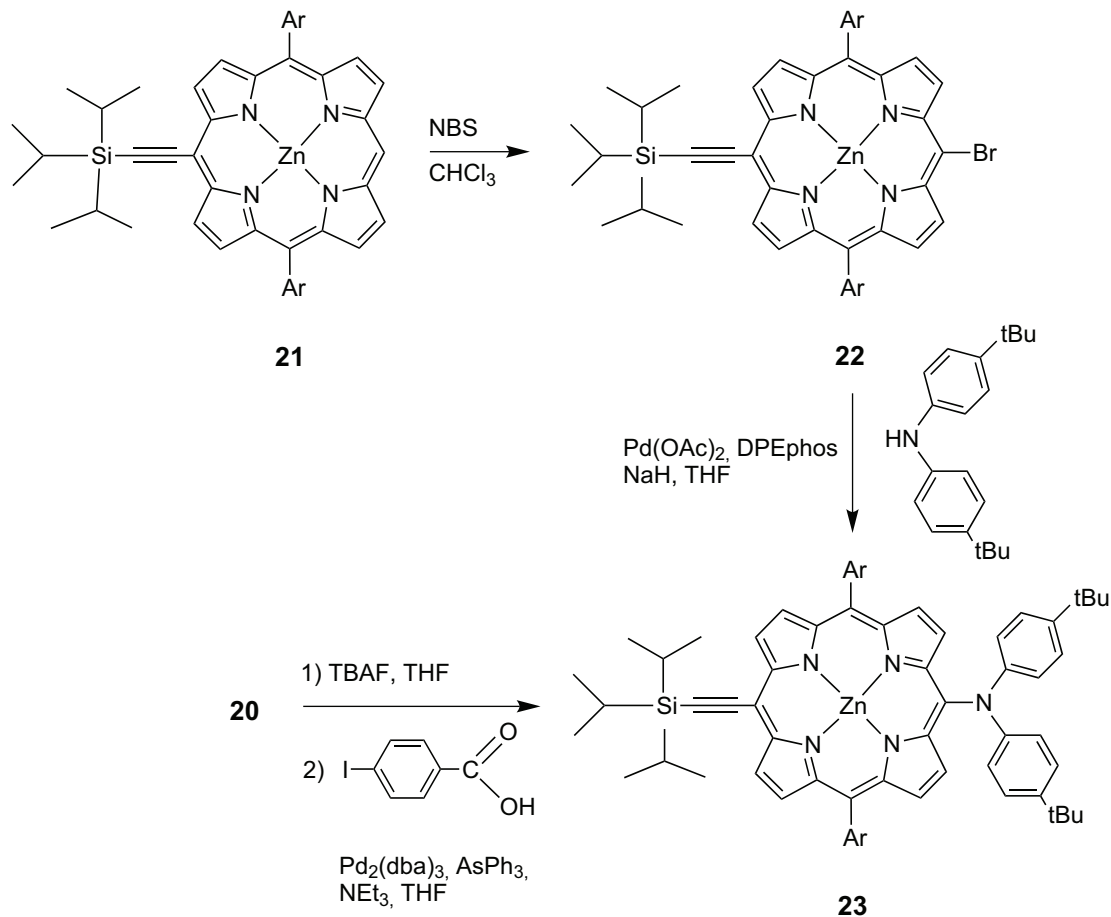


Scheme 4.

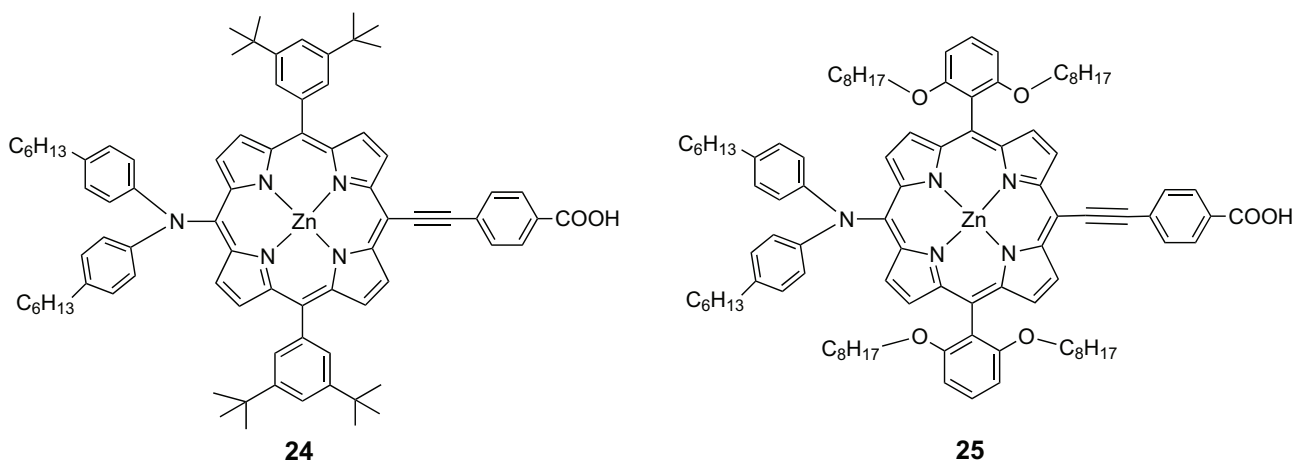
Porphyrin **20** substituted with a diarylamine group at the *meso* position was prepared according to the route detailed in Scheme 5. Bromination of **21** with NBS led to **22** and subsequent catalytic amination with bis(4-*tert*-butylphenyl)amine gave **23**. The deprotection of **23** with TBAF followed by Sonogashira coupling with *p*-iodobenzoic acid produced the target derivative **20**.

The push-pull zinc porphyrin **20** exhibited remarkable cell performances: an overall conversion efficiency ( $\eta$ ) of 6% was obtained for this dye-modified TiO<sub>2</sub> film. This conversion efficiency is higher than that of **10** (2.4%). Thus, the capabilities of light harvesting and charge separation of porphyrin dyes were clearly increased by introduction of a donor group at the *meso* position. Other molecular structures of push-pull zinc porphyrins were synthesized and studied in DSSCs by the groups of Yeh and Diau.<sup>29,30</sup> Some of the studied systems exhibited excellent cell performances and outperformed **20**-based DSSCs. However, for all these sensitizers, conversion efficiencies remained below 8%. The only exception was the porphyrin dye **24**, which exhibited PCE of 11% when used with iodide/triiodide redox electrolyte (Scheme 6). This dye contains a diarylamine group attached to the porphyrin macrocycle acting as an electron donor and an ethynylbenzoic acid moiety that serves as an electron acceptor and anchoring group. The porphyrin chromophore constitutes the bridge between the acceptor and the donor ends of the molecular system. The derivative **25** reported by the groups of Gratzel, Yeh, and Diau contains 2 octyloxy groups in *ortho* positions of each *meso*-phenyl ring.<sup>16</sup> This compound has been designed on the basis of data suggesting that the introduction of a long-chain alkyloxy group in a dye structure

may retard the unwanted charge recombination process. The photo-induced charge separation in DSSCs using Co(II/III) tris(bipyridyl) based redox electrolyte is clearly improved since an efficiency of 12.3% was observed. The PCE even exceeds 13% under air mass (AM) 1.5 solar light of  $500 \text{ W/m}^2$  intensity.



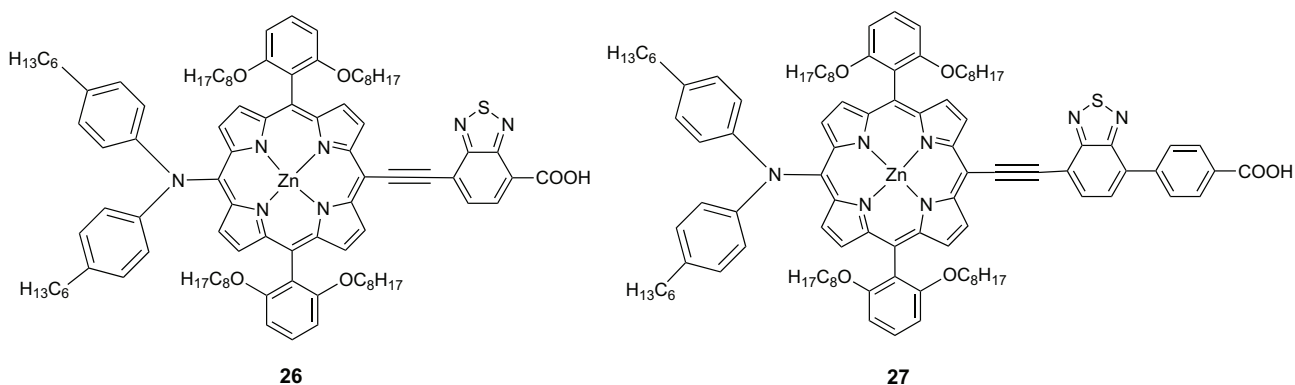
Scheme 5.



Scheme 6.



Yeh and Grätzel have very recently developed another molecular engineering of push-pull porphyrin dyes (Scheme 7).<sup>31</sup> They introduced 2,1,3-benzothiazole as a  $\pi$ -conjugated linker between the anchoring group and the porphyrin chromophore to broaden the absorption spectrum and to fill the valley between the Soret and Q bands. A power conversion efficiency of 12.75% was observed for **27** under simulated one-sun illumination. The lower PCE value observed for **26** (2.52%) is due to the absence of a phenyl group between benzothiazole and carboxylic acid groups. This induces a higher recombination chemical capacitance, inducing deeper trap states and consequently a lower  $V_{OC}$  value.



Scheme 7.

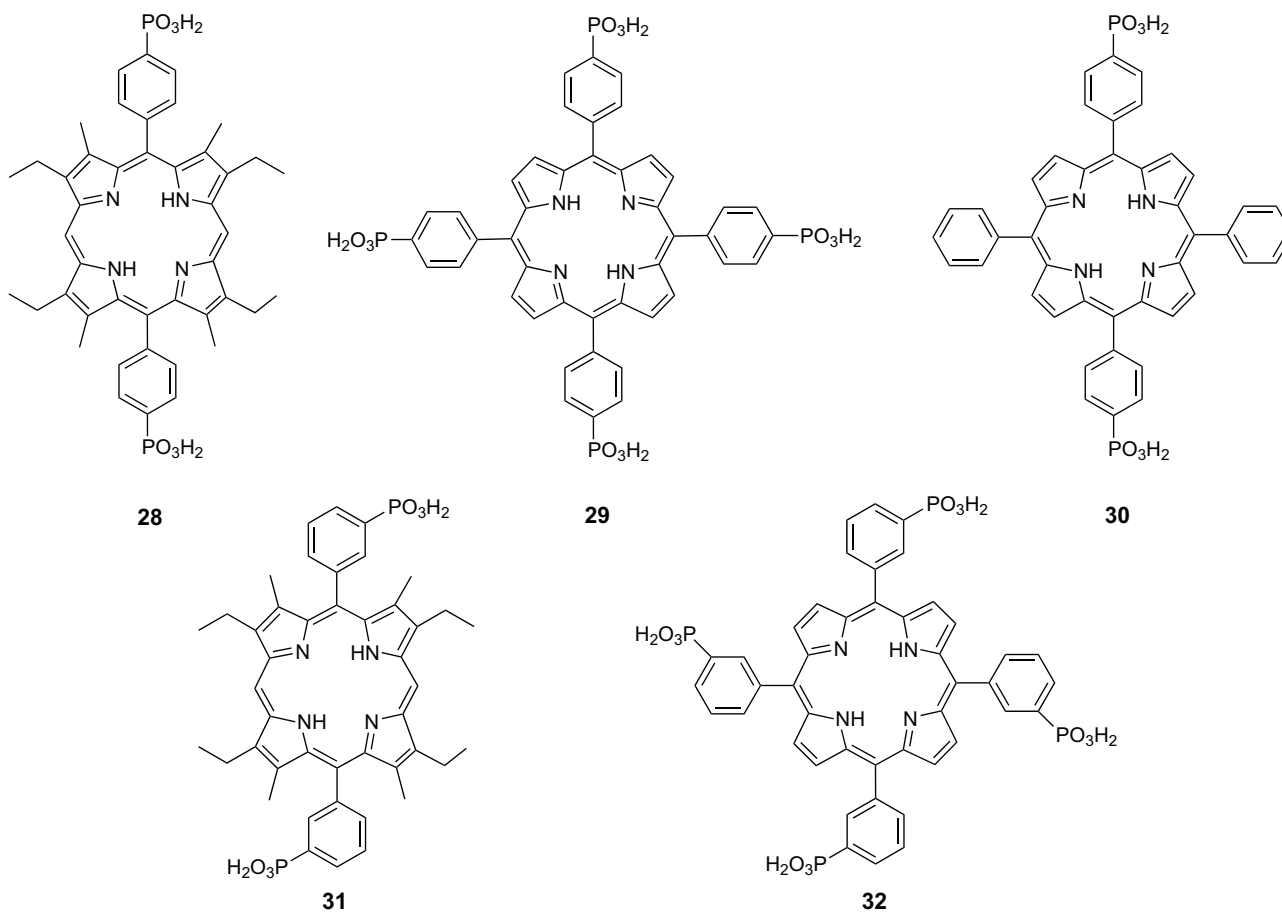
## 7. Anchoring phosphonate groups at the *meso* position of porphyrin dyes

Odobel and coworkers have prepared a series of porphyrins sensitizers (**28–32**) where the phosphonic group was the anchoring entity (Scheme 8).<sup>32</sup>

These dyes were studied by various techniques including electrochemistry and photo-electrochemical spectroscopy (Table 5). The authors have shown that the nature of the anchoring group (phosphonic or carboxylic acids) has little impact on the photo-electrochemical performance of the cell, but the substitution position of the anchoring group at the periphery of the macrocycle has a major effect on the monochromatic photon-to-electron conversion efficiency of the cell. The highest ICPE has been observed for the  $A_2B_2$  disubstituted porphyrin **31**. The authors suggest that the porphyrin bearing phosphonic acid groups in *meta* positions on the phenyl ring lies closer to the  $TiO_2$  surface than those with *para*-substituent. This influences the magnitude of the electron coupling, which is responsible for the difference in PCE observed between dyes **28** and **31**. This explains also why the activated electron transfer for dyes **29** and **32** induces similar IPCE values.

**Table 5.** Redox and photochemical properties of the porphyrins sensitizers.

Compound	$E_{1/2}/V$ vs. SCE	$E_{pa} - E_{pc}/V$	$E_{ox}/V$ vs. SCE	Max IPCE on Soret Band (%)
<b>28</b>	0.87	0.13	-1.09	9
<b>29</b>	1.13	0.16	-0.76	8
<b>30</b>	1.04	0.12	-0.83	5
<b>31</b>	0.86	0.12	-0.90	21
<b>32</b>	1.08	0.11	-0.80	8



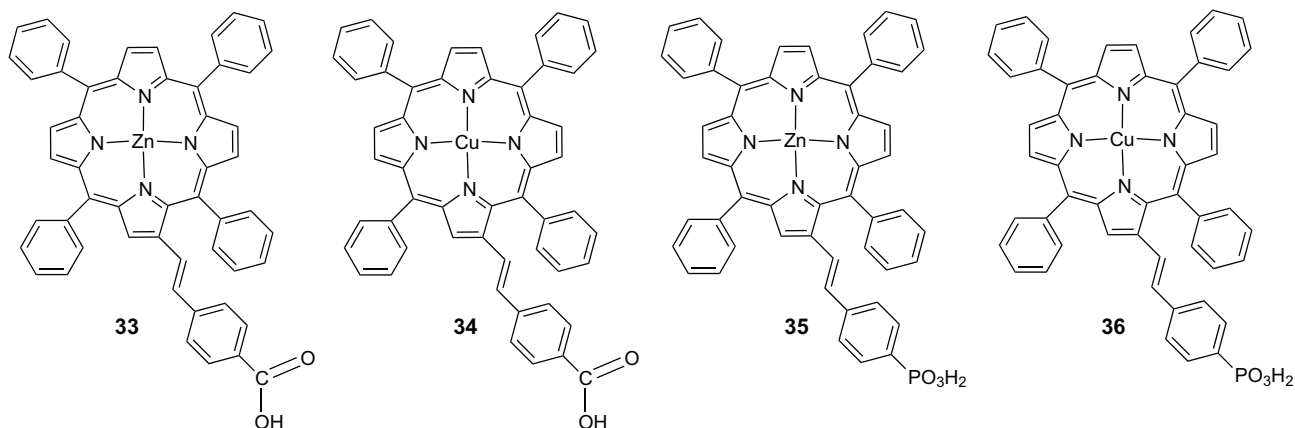
Scheme 8.

### 8. Effect of anchoring groups: phosphonate versus carboxylate linkages in porphyrin series

In 2004 Grätzel and coworkers studied a series of carboxylic and phosphonic metalloporphyrins to evaluate absorption and photovoltaic properties in  $\text{TiO}_2$ -nanocrystalline DSSCs. The studied metalloporphyrins were all  $\beta$ -linked alkenyl benzoic acid ethers or their phosphorus analogues.<sup>17</sup> This comparative study led to 2 main conclusions (Table 6): 1) the diamagnetic metalloporphyrins exhibit higher incident monochromatic photon-to-current conversion compared to the corresponding paramagnetic copper porphyrins; 2) metalloporphyrins bearing a phosphonate anchoring group show lower efficiencies than those bearing a carboxylate anchoring group in this series.

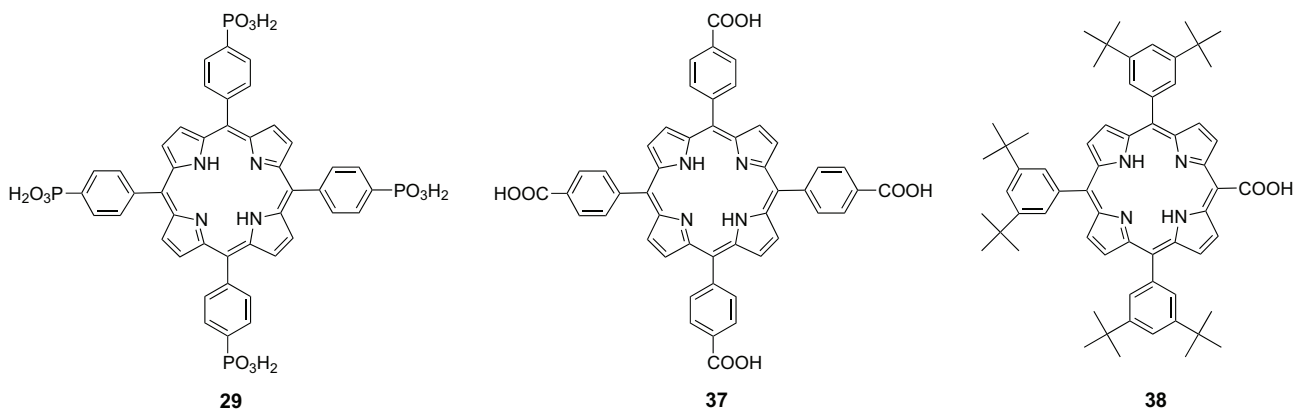
Odobel and coworkers have discussed the relative photo-electrochemical performances of sensitizers bearing phosphonic and carboxylic groups anchored at the *para*-positions of *meso*-phenyl groups (Table 7).<sup>32</sup> The performances of the phosphonic derivatives are close to those of the carboxylic derivatives. A high performance is observed for dye **38** bearing the  $\text{COOH}$  anchoring directly bonded to the  $\pi$  aromatic macrocycles. This result has been attributed to a stronger interaction with  $\text{TiO}_2$  compared to sensitizer **37** where the  $\text{COOH}$  motifs are electronically decoupled from the porphyrin core.

The groups of Gust and Moore have shown that porphyrin dyes bearing  $\beta$ -vinyl substituents with carboxylic acid or phosphonic acid demonstrate similar photophysical properties (Table 8).<sup>33</sup> These derivatives

**Table 6.** Photovoltaic performance of nanocrystalline TiO<sub>2</sub> films sensitized by porphyrins dyes using electrolyte 1376.<sup>a</sup>

Complex	Solution	IPCE at $\lambda$	$I_{SC}$ (mA/cm <sup>2</sup> )	$V_{OC}$ (mV)	FF	Efficiency under 1 sun
		450 nm (%)				
<b>33</b>	THF	73	8.86	654	0.71	4.11
<b>34</b>	THF	5	1.35	490	0.69	0.45
<b>35</b>	THF	30	2.05	580	0.75	0.89
<b>36</b>	THF	4	1.1	561	0.67	0.71

<sup>a</sup> The composition of electrolyte 1376 is 0.6 M butylmethimidazolium iodide (BMII), 0.05 M I<sub>2</sub>, 0.1 M LiI, and 0.5 M *tert*-butylpyridine in 1:1 acetonitrile and valeronitrile.

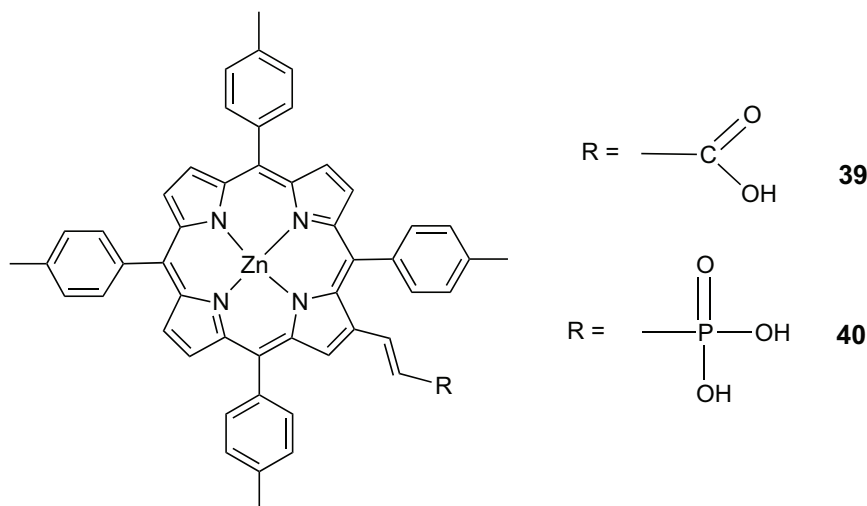
**Table 7.** Redox and photochemical properties of the porphyrin sensitizers.

	$E_{1/2}$ /V vs. SCE	$E_{pa} - E_{pc}$ /V	$E_{OX}$ /V vs. SCE	Max IPCE on Soret Band (%)
<b>29</b>	1.13	0.16	-0.76	8
<b>37</b>	1.10	0.10	-0.74	10
<b>38</b>	1.06	0.13	-0.79	17

attached to anatase TiO<sub>2</sub> nanoparticles show a different surface covering: the coverage obtained with the carboxylic acid derivative is about twice higher of those of the phosphonic acid. This difference was attributed to the geometry of the anchoring groups on the TiO<sub>2</sub> surface. It can be noted that for DSSCs the values of  $V_{OC}$  and FF are similar for the 2 linkers but the short-circuit current and solar conversion efficiency of the

cell with the carboxylic linker were about twice those observed with the phosphonic acid dye. The highest values observed for the carboxylic acid sensitizer result from the increased surface coverage. Comparison of the stability of the 2 derivatives under basic conditions shows that the carboxylate is readily hydrolyzed, while the phosphonate linkages are much less labile.

**Table 8.** Performances of DSSCs.<sup>a</sup>



Porphyrin	$J_{SC}$ (mA/cm <sup>2</sup> )	$V_{OC}$ (mV)	FF	PCE (%)
<b>39</b>	2.49	444	0.52	0.57
<b>40</b>	1.11	426	0.53	0.25

<sup>a</sup> Illuminated using simulated AM 1.5 G sunlight at 1000 W/m<sup>2</sup>.

## 9. Conclusions and perspectives

We have detailed in a previous review new methodologies of synthesis of phosphonate derivatives of porphyrins or metalloporphyrins.<sup>9</sup> The present review has been dedicated to establish the effect of the anchoring group nature in porphyrin sensitizers mainly based on comparative studies of phosphonate versus carboxylate linkages.

Numerous works on the development of photovoltaic and photocatalytic systems using solar energy have been described. Three main processes govern the light energy conversion: light-harvesting and exciton diffusion, charge separation, and carrier transport. Moreover, for photocatalytic systems 3 main components are also needed: the photosensitizer, the electron relay, and the catalyst. For both applications, light absorption and the subsequent electron transfer through the excited state are the key processes for the final energy conversion.

Various techniques are currently developed to allow a high module efficiency and a very low cost of production for organic solar cells based on porphyrins and metalloporphyrins. The key problem is to improve the stability of the modules. The search for new solutions by the use of self-organization and the control of self-assembly should be the way to achieve stepwise progress. Recent developments in synthetic and supramolecular techniques have made it possible to control, organize, and arrange molecules at the nanometer level. In photovoltaic cells, the construction of supramolecular photofunctional materials for light energy conversion must lead to major enhancements of light energy conversion properties as compared to the nonorganized systems. Therefore, a powerful strategy is to develop building blocks allowing a precise alignment onto the surface electrode using a patterning technique. We are confident that the supramolecular strategies will pave the way for the development of light energy conversion systems.

As an example, we have shown that the phosphoryl substituted porphyrins are particularly versatile organic precursors for elaboration of functional hybrid organic/inorganic materials having a great variety of structure types. Moreover, as shown in this review, the phosphonate linkage is much less labile than the carboxylate one in various experimental conditions.

In another domain the use of the phosphonate anchoring group is challenging to develop efficient multi-electron catalysts that exhibit strong stability in aqueous media.

### Acknowledgments

This work was performed in the frame of the French-Russian Associated Laboratory “LAMREM” supported by the CNRS and the Russian Academy of Sciences, Russian Foundation for Basic Research (grant #12-03-93110).

### List of Abbreviations

AM	Air Mass
APCE	Adsorbed-Photon-to-Current Efficiency
DSSCs	Dye-Sensitized Solar Cells
FF	Fill Factor
IPCE	Incident-Photon-to-Current Efficiency
$I_{SC}$	Short Circuit Photocurrent
$J_{SC}$	Photocurrent Density
PCE or $\eta$	Power Conversion Efficiency (derived from $\eta = J_{SC} \times V_{OC} \times FF$ )
$V_{OC}$	Open Circuit Voltage

### References

1. Campbell, W. M.; Burrell, A. K.; Officer, D. L.; Jolley, K. W. *Coord. Chem. Rev.* **2004**, *248*, 1363–1379.
2. Martinez-Diaz, M. V.; de la Torre, G.; Torres, T. *Chem. Commun.* **2010**, *46*, 7090–7108.
3. Wang, X.-F.; Tamiaki, H. *Energy Environ. Sci.* **2010**, *3*, 94–106.
4. Hagfeldt, A.; Boschloo, G.; Sun, L.; Kloo, L.; Pettersson, H. *Chem. Rev.* **2010**, *110*, 6595–6663.
5. Walter, M. G.; Rudine, A. B.; Wamser, C. C. *J. Porphyrins Phthalocyanines* **2010**, *14*, 759–792.
6. Nazeeruddin, M. K.; Baranoff, E.; Gratzel, M. *Sol. Energy* **2011**, *85*, 1172–1178.
7. Panda, M. K.; Ladomenou, K.; Coutsolelos, A. G. *Coord. Chem. Rev.* **2012**, *256*, 2601–2627.
8. Li, L.-L.; Diau, E. W.-G. *Chem. Soc. Rev.* **2013**, *42*, 291–304.
9. Bessmertnykh Lemeune, A. G.; Stern, C.; Gorbunova, Y. G.; Tsivadze, A. Y.; Guilard, R. *Macroheterocycles* **2014**, *7*, 122–132.
10. Enakieva, Y. Y.; Bessmertnykh, A. G.; Gorbunova, Y. G.; Stern, C.; Rousselin, Y.; Tsivadze, A. Y.; Guilard, R. *Org. Lett.* **2009**, *11*, 3842–3845.
11. Kadish, K. M.; Chen, P.; Enakieva, Y. Y.; Nefedov, S. E.; Gorbunova, Y. G.; Tsivadze, A. Y.; Bessmertnykh-Lemeune, A.; Stern, C.; Guilard, R. *J. Electroanal. Chem.* **2011**, *656*, 61–71.
12. Sinelshchikova, A. A.; Nefedov, S. E.; Enakieva, Y. Y.; Gorbunova, Y. G.; Tsivadze, A. Y.; Kadish, K. M.; Chen, P.; Bessmertnykh-Lemeune, A.; Stern, C.; Guilard, R., *Inorg. Chem.* **2013**, *52*, 999–1008.
13. Zubatyuk, R.I.; Sinelshchikova, A.A.; Enakieva, Y.Y.; Gorbunova, Y.G.; Tsivadze, A.Y.; Nefedov, S.E.; Bessmertnykh-Lemeune, A.; Guilard, R.; Shishkin, O.V. *Cryst.Eng.Comm.*, **2014**, in print.
14. Vinogradova, E. V.; Enakieva, Y. Y.; Nefedov, S. E.; Birin, K. P.; Tsivadze, A. Y.; Gorbunova, Y. G.; Lemeune Bessmertnykh, A.; Stern, C.; Guilard, R. *Chem. Eur. J.* **2012**, 15092–15104.

15. Fang, Y. Y.; Kadish, K. M.; Chen, P.; Gorbunova, Y.; Enakieva, Y.; Tsvadze, A.; Bessmertnykh-Lemeune, A.; Guillard, R. *J. Porphyrins Phthalocyanines* **2013**, *17*, 1035–1045.
16. Yella, A.; Lee, H. W.; Tsao, H. N.; Yi, C. Y.; Chandiran, A. K.; Nazeeruddin, M. K.; Diau, E. W. G.; Yeh, C. Y.; Zakeeruddin, S. M.; Gratzel, M. *Science* **2011**, *334*, 629–634.
17. Nazeeruddin, M. K.; Humphry-Baker, R.; Officer, D. L.; Campbell, W. M.; Burrell, A. K.; Grätzel, M. *Langmuir* **2004**, *20*, 6514–6517.
18. Vioux, A.; Le Bideau, J.; Mutin, P. H.; Leclercq, D. *Top. Curr. Chem.* **2004**, *232*, 145–174.
19. Ukaji, E.; Furusawa, T.; Sato, M.; Suzuki, N. *Appl. Surf. Sci.* **2007**, *254*, 563–569.
20. Ooyama, Y.; Nagano, T.; Inoue, S.; Imae, I.; Komaguchi, K.; Ohshita, J.; Harima, Y. *Chem. Eur. J.* **2011**, *17*, 14837–14843.
21. Ma, T.; Inoue, K.; Noma, H.; Yao, K.; Abe, E. *J. Photochem. Photobiol., A* **2002**, *152*, 207–212.
22. He, H.; Gurung, A.; Si, L. *Chem. Commun.* **2012**, *48*, 5910–5912.
23. Bae, E. Y.; Choi, W. Y.; Park, J. W.; Shin, H. S.; Kim, S. B.; Lee, J. S. *J. Phys. Chem. B* **2004**, *108*, 14093–14101.
24. Park, H.; Bae, E.; Lee, J. J.; Park, J.; Choi, W. *J. Phys. Chem. B* **2006**, *110*, 8740–8749.
25. Imahori, H.; Hayashi, S.; Hayashi, H.; Oguro, A.; Eu, S.; Umeyama, T.; Matano, Y. *J. Phys. Chem. C* **2009**, *113*, 18406–18413.
26. Hart, A. S.; Chandra, B. K. C.; Gobeze, H. B.; Sequeira, L. R.; D'Souza, F. *ACS Appl. Mater. Inter.* **2013**, *5*, 5314–5323.
27. Park, J. K.; Lee, H. R.; Chen, J. P.; Shinokubo, H.; Osuka, A.; Kim, D. *J. Phys. Chem. C* **2008**, *112*, 16691–16699.
28. Lee, C. W.; Lu, H. P.; Lan, C. M.; Huang, Y. L.; Liang, Y. R.; Yen, W. N.; Liu, Y. C.; Lin, Y. S.; Diau, E. W. G.; Yeh, C. Y. *Chem. Eur. J.* **2009**, *15*, 1403–1412.
29. Lu, H. P.; Tsai, C. Y.; Yen, W. N.; Hsieh, C. P.; Lee, C. W.; Yeh, C. Y.; Diau, E. W. G. *J. Phys. Chem. C* **2009**, *113*, 20990–20997.
30. Hsieh, C. P.; Lu, H. P.; Chiu, C. L.; Lee, C. W.; Chuang, S. H.; Mai, C. L.; Yen, W. N.; Hsu, S. J.; Diau, E. W. G.; Yeh, C. Y. *J. Mater. Chem.* **2010**, *20*, 1127–1134.
31. Yella, A.; Mai, C. L.; Zakeeruddin, S. M.; Chang, S. N.; Hsieh, C. H.; Yeh, C. Y.; Gratzel, M. *Angew. Chem., Int. Ed.* **2014**, *53*, 2973–2977.
32. Odobel, F.; Blart, E.; Lagree, M.; Villieras, M.; Boujtita, H.; El Murr, N.; Caramori, S.; Bignozzi, C. A. *J. Mater. Chem.* **2003**, *13*, 502–510.
33. Brennan, B. J.; Llansola Portoles, M. J.; Liddell, P. A.; Moore, T. A.; Moore, A. L.; Gust, D. *Phys. Chem. Chem. Phys.* **2013**, *15*, 16605–16614.